

结构化填充床内层流流动特性的研究

李楠¹, 史俊瑞¹, 刘洋¹, 冷杰²

(1. 沈阳工程学院 沈阳市循环流化床燃烧技术重点实验室 辽宁 沈阳 110136;

2. 东北电力科学研究院有限公司 辽宁 沈阳 110006)

摘要: 本文对填充床内顺序排列, 六层堆积的直径为 28 mm 的八分之一小球的流动特性进行数值研究, 定量分析孔隙内的流动特性, 并详细研究了颗粒 Re 数的变化对多孔介质内层流流场的影响。结果表明, 当颗粒 Re 为 12.17 和 28.88 时, 流线贴着小球壁面流动; 当颗粒 Re 为 105.57 和 204.74 时, 由于惯性力的影响占了主导作用, 流线不再贴着小球壁面流动, 同时, 当颗粒 Re 为 204.74 时, 在孔隙内部产生了明显的回流现象。

关键词: 多孔介质; 数值模拟; 流场; 填充床

中图分类号: TQ051.1 文献标识码: A

DOI: 10.16146/j.cnki.rndlge.2016.10.014

引言

多孔介质中的对流换热现象一直备受关注, 填充床作为一类典型的多孔介质, 其内部进行着复杂的流动及传热传质等过程, 广泛的应用于冶金、化工和蓄热发电等领域。由于非结构化填充床内部流动阻力大且综合换热效率较低, 因此, 结构化填充床受到越来越多的关注^[1-3]。

实验研究通常采用 CT 扫描、核磁共振成像等方法来获得填充床内部真实的小球结构^[4-5], 并观察流场内部参数变化对流场的影响; Suekane 等采用核磁共振成像技术, 研究了填充床内部流场由惯性流转化为层流时内部的速度分布规律^[5]。根据颗粒 Re 数的不同, 有 4 种流动机理: 蠕动流动 ($Re < 1$)、惯性流动 ($1 < Re < 150$)、不稳定层流 ($150 < Re < 300$) 和高度不稳定流 ($Re > 300$)。但由于受到实验设备以及成本的限制, 并不能观察到沿着主流方向整个流场流线的特性。随着高性能计算机水平的高速发展和数值计算的涌现, 数值模拟方法已经成为揭示孔隙内部流动和与换热规律的有效

手段^[6-7]。

本研究采用 CFD(计算流体力学)方法, 对三维小球有序排列多孔介质孔隙的流动进行了数值研究, 详细的分析了 Re 的变化对孔隙内部流场流线的影响, 为深入研究多孔介质内部流动规律提供理论依据。

1 物理模型

本模拟以 Suekane 等实验研究的简单立方体有序排列的填充床为物理模型^[5], 填充床通道由六层小球堆积而成, 构成 5 个简单立方体, 每个立方体由 8 个八分之一小球组成, 小球直径为 28 mm, 通道总长度为 168 mm, 孔隙率为 0.476, 如图 1(a) 所示。为了避免在小球接触点附近生成低质量网格, 将小球的直径缩为 $0.99d$ (d 为小球直径), 小球与小球的间隙为 $0.01d$, 此时孔隙率为 0.491。根据文献 [6] 在层流状态下, 采用该方法对流动过程模拟结果的影响很小。为了消除进出口边界效应对模拟结果的影响, 计算区域分别向主流方向的上游和下游各伸长 3 个小球直径长度, 总的计算区域的长度为 336 mm。同时, 由于计算条件有限, 对所描述的三维填充床内多孔介质孔隙内的流动实施全场模拟尚不可行, 且小球的排列通道沿 x 轴、 y 轴对称, 因此, 本文选取小球的 1/4 通道(沿 x 和 y 方向)作为数值模拟的计算区域, 如图 1(b) 所示。

2 控制方程

本文限定研究范围颗粒 Re 小于 300 的场合, 流动速度较小, 假设流体流动为层流且不可压缩。

收稿日期: 2015-12-15; 修订日期: 2015-12-22

基金项目: 国家自然科学基金(50476105, 51406123); 沈阳工程学院校内科技基金项目(LGQN-1503)

作者简介: 李楠(1985-), 女, 辽宁营口人, 沈阳工程学院工程师。

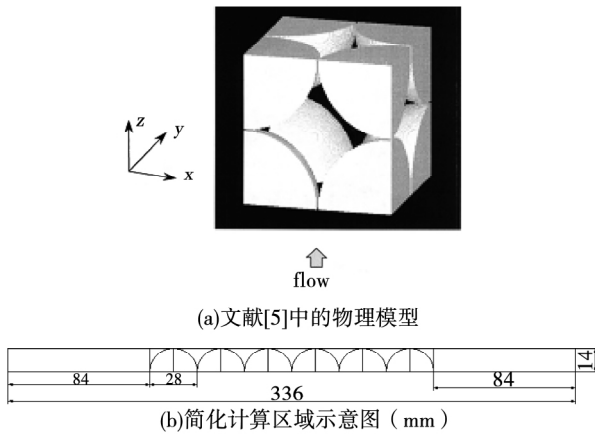


图 1 简化计算区域示意图
Fig. 1 Simplified Schematic diagram of calculation domain

2.1 控制方程

连续性方程:

$$\nabla(\rho_g \bar{v}) = 0 \quad (1)$$

式中: ρ_g —水的密度 kg/m^3 ; \bar{v} —流体速度矢量。

动量方程:

$$\nabla(\rho_g \bar{v}\bar{v}) = -\nabla P + \mu \nabla(\nabla \bar{v}) \quad (2)$$

2.2 边界条件

Suekane 等的填充床为对称结构^[5],为节省计算资源,沿着流动方向取其中的四分之一作为计算域,即假设对称边界条件。

边界条件如下:

$$\left\{ \begin{array}{l} z = 0 \quad T = T_0 \quad \nu_x = \nu_y = 0 \quad \nu_z = \nu_{z,0} \\ z = L \quad \frac{\partial \nu_x}{\partial z} = \frac{\partial \nu_y}{\partial z} = \frac{\partial \nu_z}{\partial z} = 0 \\ x = 0 \quad H/2 \quad \frac{\partial \nu_y}{\partial x} = \frac{\partial \nu_z}{\partial x} = 0 \quad \nu_x = 0 \\ y = 0 \quad H/2 \quad \frac{\partial \nu_x}{\partial y} = \frac{\partial \nu_z}{\partial y} = 0 \quad \nu_y = 0 \\ \text{颗粒壁面} \quad \nu_x = \nu_y = \nu_z = 0 \end{array} \right. \quad (3)$$

式中: ν_x, ν_y, ν_z —速度分量; T —温度, K。

2.3 求解

首先对所研究的问题进行网格无关性考核,在不同的网格数量下,对简单立方体内的流动进行考核。采用非结构化的四面体网格,对计算区域进行划分。同时,由于局部孔隙间距狭小,采用 size-function 方法,对孔隙的网格进行加密处理,如图 2 所示。网格数量共计 258 万,并获得了相应的无了解。基于压力-速度耦合 SIMPLE 算法进行计算。

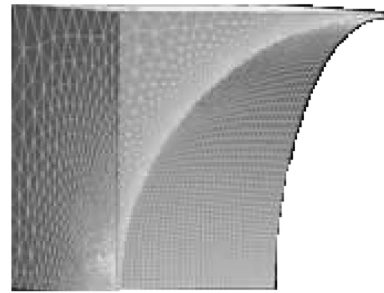
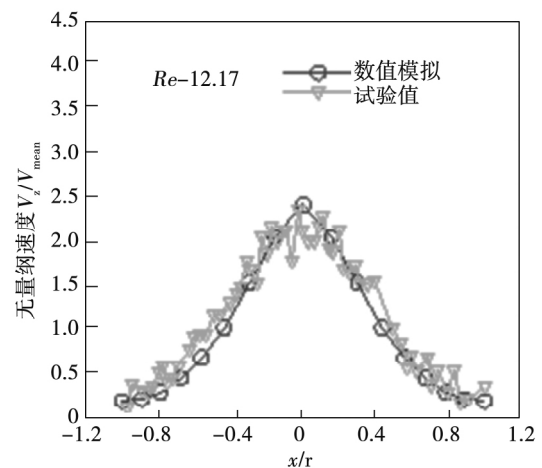
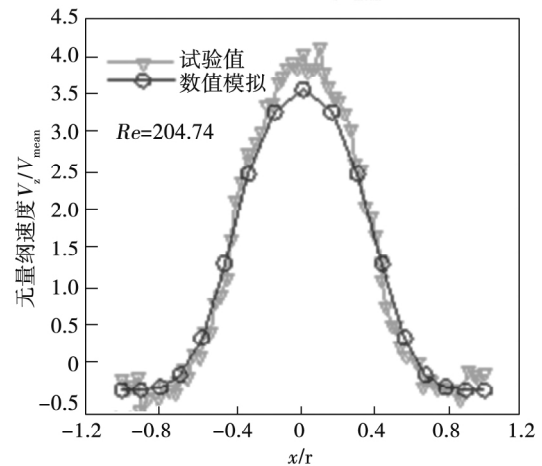


图 2 单元体网格划分
Fig. 2 Mesh of unit cell



(a) $Re=12.17$ 沿 x 轴 v_z/v_{mean} 分布



(b) $Re=204.74$ 沿 x 轴 v_z/v_{mean} 分布

图 3 $Re = 204.74$ 沿 x 轴 v_z/v_{mean} 分布

Fig. 3 v_i/v_{mean} distribution along x -axis ($Re = 204.74$)

3 结果与分析

3.1 数值模型的验证

图 3 为颗粒 Re 为 12.17 和 204.74 时,在第 4

个单元体中心 ($y = 0.014 \text{ m}$, $z = 0.196 \text{ m}$) 沿 x 轴的 z 方向无量纲速度 (v_z/v_{mean}) 实验值与模拟值的分布曲线。其中 v_{mean} 表示平均速度, $v_{\text{mean}} = Q/A\varepsilon$, Q 指通过单元体的体积流量, A 指单元体的横截面积, ε 指孔隙率。从图中可以看出, 模拟数据与实验值吻合的较好。沿着 x 轴的正负方向, 速度分布成抛物线形式。当 Re 为 12.17 时, 沿着 x 轴流速在单元体中心速度最大, 从单元体中心到小球壁面, 速度逐渐减小, 但流速变化较为平缓, 最大值在 2.5 左右。当 Re 为 204.74 时, 沿着 x 轴从单元体中心到小球壁面, 流速变化较大, 最大值在 4 左右。在 $x/r = 0$ 处, 实验值略高于模拟值, 在 $x/r = 0.8$ 处, 实验值和模拟值都显示出了负数, 说明此时产生了回流。总之,

模拟值与实验值吻合的结果较好, 从定量角度验证了模拟的准确性。

图 4 为 Re 为 204.74 时, 流体经过第 4 个单元体时, 沿着流动方向 A、B 和 C 3 个垂直切面上实验和模拟的速度矢量的对比图。通过数值模拟可以看出, 当流体流经切面 A 时, 产生了漩涡, 同时试验测量也观察到了此现象。当流体流经切面 B 和 C 时, 流体都是沿着小球壁面的方向进行流动。图 3 和图 4 分别从定量和定性两个角度验证了模拟值与实验值的一致性。模拟结果不仅反映了沿着流动方向上流速的大小, 同时准确的捕捉到了流场内部的流动特性。因此, 本文利用数值模拟研究随着颗粒 Re 的变化, 结构化填充床内部流场的流动特性。

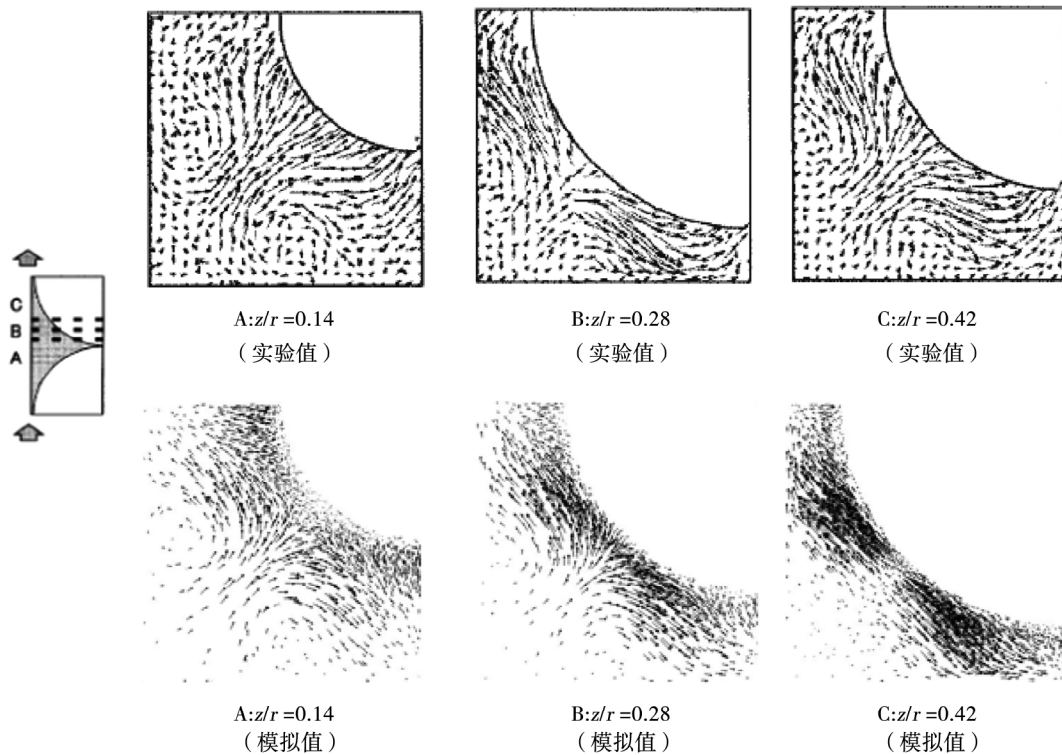


图 4 垂直于 Z 轴的 3 个切面上实验值与模拟值的对比图 ($Re = 204.74$)

Fig. 4 Comparison of the simulated flow field with experimental data at three horizontal planes ($Re = 204.74$)

3.2 速度矢量图表征单元体流动特性

图 5 为不同 Re 时, 沿着主流方向流体流经第 4 个单元体时的速度矢量图。从图中可以看出, 当 Re 为 12.17 和 28.88 时, 经过单元体中心区域时, 流体的流线分成二部分, 一部分沿着主流方向, 平行于 z 轴进行流动; 另一部分流体贴着小球的壁面流动, 这

主要由于 Re 较小时, 粘性力起着主导作用。当 Re 为 59.78 时, 仍有一部分流体贴着壁面进行流动, 但对小球壁面的附着程度在减小, 说明粘性力的作用在减小, 而惯性力的作用在增加。当 Re 为 105.57 和 204.74 时, 流线不再贴着小球壁面流动, 基本上都平行于 z 轴, 说明这时惯性力起着主导作用。同时,

当 Re 为 204.74 时, 流线以射流的方式沿着主流方向流动, 并在孔隙区间产生了漩涡, 变成了不稳定的层流。

3.3 流线表征流场流动特性

图 6 为不同 Re 时, 流体沿着主流方向流经流场的速度变化图。从图中可以看出, 当 Re 为 12.17 和 28.88 时, 随着流通面积的增大, 平行于 z 轴的流体流速逐渐减小, 当流通面积减小时, 流速又变大。在间隙最小处, 流速达到最大值, 且最大值和最小值相差较多。同时在间隙最小处, Re 为 28.88 时的无量纲速度看起来比 Re 为 12.17 时大, 实际上当 Re 为 12.17 时, 无量纲速度也能达到最大值 5 左右。由于流线图 n 条流线叠加而成, 根据文献 [5] 可知, 当

Re 为 12.17 时, 通入流量 Q 为 $162.21 \text{ mm}^3/\text{s}$, 当 $Re = 28.88$ 时流量 Q 为 $384.9 \text{ mm}^3/\text{s}$ 。因此, 当 Re 为 12.17 时, 流量相对较少且流体主要贴着壁面流动, 在此处平行于 z 轴的流线较少, 所以流线叠加起来的颜色没有 Re 为 28.8 时的颜色红。当 Re 为 59.78 时, 流速在间隙最大和最小处的差距逐渐减小, 说明随着 Re 的增加, 惯性力的作用越来越大, 所以速度经过叠加后, 整个流体区域的流速差别逐渐减小。当 Re 为 105.57 和 204.74 时, 流速在整个流动区间几乎不变, 并且当 Re 为 204.74 时, 在流场的每个流通面积最大处产生了涡流, 也因此在此图 3(b) 中 $x/r = 0.8$ 处产生了负值。

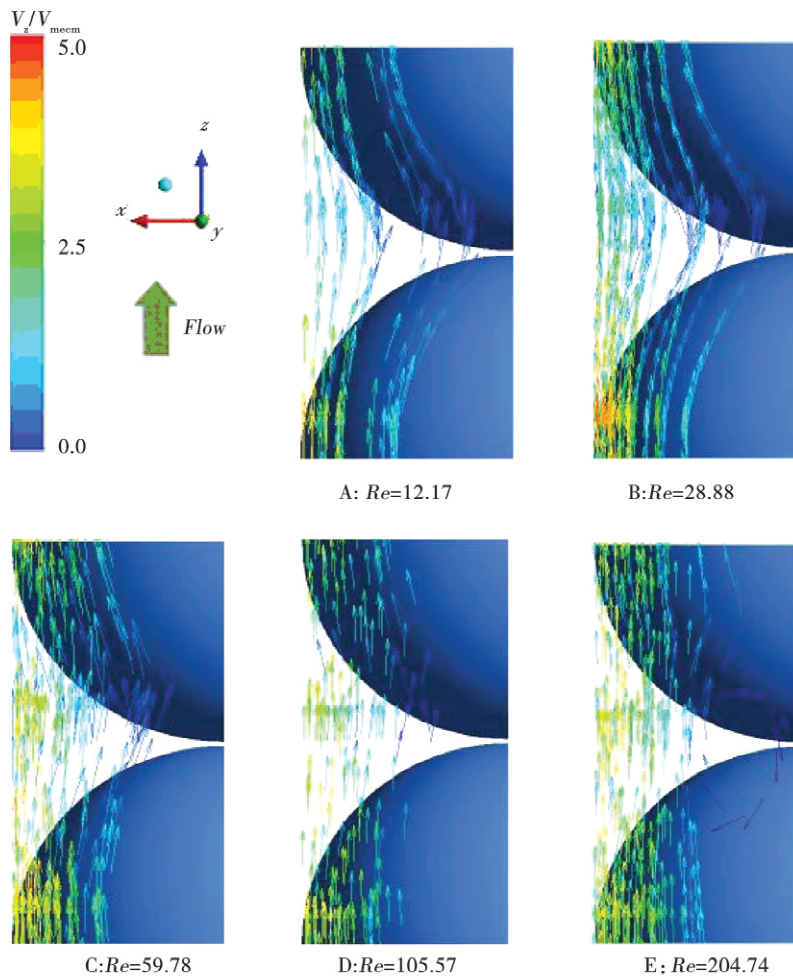
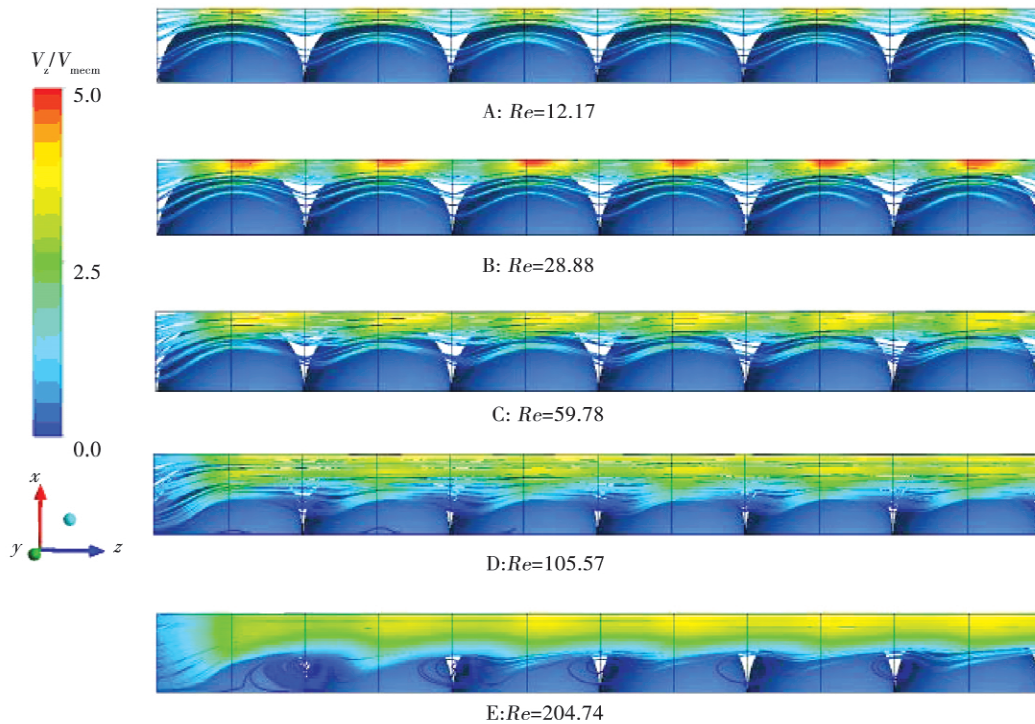


图 5 不同 Re 数时流体流经单元体的速度矢量图

Fig. 5 Velocity vector with different Re numbers

图 6 不同 Re 时流场的流线图Fig. 6 Flow field with different Re numbers

4 结 论

(1) 在层流范围内, 当 Re 较小时, 沿着主流方向, 流体贴着壁面进行流动, 这时粘性力起着主要作用。但随着 Re 的增大, 对壁面的附着程度越来越小, 当 Re 为 204.74 时, 流体不再贴着小球壁面, 而是以射流的方式流出, 此时惯性力起着主要作用;

(2) 当 Re 较小时, 沿着主流方向, 在间隙最小处, 速度较大, 间隙最大处, 流速较小, 随着 Re 的增大, 二者之间的差距逐渐减小, 当 Re 为 204.74 时, 整个流场的速度几乎不变。

参考文献:

- [1] NIJEMEISLAND M, DIXON A G. Comparison of CFD simulation to experiment for convective heat transfer in a gas-solid fixed bed [J]. *Chemical Engineering Journal* 2001 82: 231 - 246.
- [2] YANG J, WANG Q W, ZENG M, et al. Computational study of forced convective heat transfer in structured packed beds with spherical or ellipsoidal particles [J]. *Chemical Engineering Science* 2010 65(2): 726 - 738.
- [3] 陈凯, 余钊圣, 邵雪明. 多孔介质方腔自然对流的直接数值模拟 [J]. *浙江大学学报(工学版)* 2012 46(3): 549 - 554.
- [4] CHEN Kai, YU Zhao-sheng, SHAO Xue-ming. Computational study of natural convective in a porous medium [J]. *Journal of Zhejiang University: Engineering Science* 2012 46(3): 549 - 554.
- [5] WOOD B D, APTE S V, LIBURDY J A, et al. A comparison of measured and modeled velocity fields for a laminar flow in a porous medium [J]. *Advances in Water Resources* 2015: 85: 45 - 63.
- [6] SUEKANE T, YOKOUCHI Y, HIRAI S. Inertial flow structures in a simple-packed bed of spheres [J]. *Fluid Mechanics and transport phenomena* 2003 41(9): 10 - 17.
- [7] DIXON A G, NIJEMEISLAND M, STITT E H. Systematic mesh development for 3D CFD simulation of fixed beds: contact points study [J]. *Computers and Chemical Engineering*, 2013: 48: 135 - 153.
- [8] YANG J, WANG Q W, ZENG M, et al. Computational study of forced convective heat transfer in structured packed beds with spherical or ellipsoidal particles [J]. *Chemical Engineering Science* 2010 65(2): 726 - 738.
- [9] 杨伟, 薛思瀚, 刘秦见, 等. 饱和多孔介质自然对流数学模型与实验研究 [J]. *热能动力工程* 2015 30(1): 42 - 47.
- [10] YANG Wei, XUE Si-han, LIU Qin-jian, et al. Mathematical model and experimental research of natural convection in saturated porous media [J]. *Journal of Engineering for Thermal Energy and Power*, 2015 30(1): 42 - 47.

(单丽华 编辑)

In order to enhance the pre-judgment ability of feasibility of compaction for prevention of spontaneous combustion in coal stockpiles, the simulation model of spontaneous combustion in coal stockpile has been established by using the software of COMSOL Multiphysics 5.0. Numerical simulations for 5 different stack dimensions of coal stockpile were carried out, and the changes of temperature and time of spontaneous combustion after compacting were studied and the applicability of compaction in coal stockpile were analyzed. The minimum inapplicability wind-velocity equation of coal stockpile compaction was established with the consideration of porosity. The results show that there are different minimum inapplicability wind velocities for the compaction of coal stockpile. The minimum inapplicability wind-velocity from the perspective of changes in temperature is lesser than that from the perspective of changes in time of spontaneous combustion. Set the smaller value as the judgment standard, there is a weak correlation with the stack dimensions and the minimum inapplicability wind-velocity, but it is significantly affected by the original porosity. The relationship between the minimum inapplicability wind-velocity of compaction and the original porosity of coal stockpile exhibits a power function correlation. **Key words:** spontaneous combustion of coal stockpile, compaction, inapplicability wind velocity, stack dimension, porosity

基于流场不均匀度对 SCR 效率影响的探究 = **The effect of Uneven Flow Field on the Efficiency of SCR**
[刊 汉] NIU Cai-wei, LIU Han-tao (School of Machinery and Power Engineering, North University of China, Taiyuan, China, Post Code: 030051) ZHANG Pei-hua (Shanxi Pingshuo Ganguo-fired Power Generation Co. Ltd., Huozhou, Post Code: 036800), JIA Jian-dong (School of Machinery and Power Engineering, North University of China, Taiyuan, China, Post Code: 030051) // Journal of Engineering for Thermal Energy & Power. - 2016, 31 (10) . - 72 ~ 78

The flow field in a selective catalytic reduction selective catalytic reduction (SCR) denitration reactor of a 600 MW coal-fired power plant was numerically simulated. Based on the relative standard deviation, the unevenness of NO and NH₃ concentration, the velocity, flue gas temperature as well as coincide trend of NO and NH₃ concentration at the entrance of the first layer of the catalyst were investigated. The results show that the unevenness of concentration and flue gas temperature are higher than other conditions, the unevenness of NO concentration, NH₃ concentration and flue gas temperature all reduced as the conditions become 50THA, 75THA, THA, BRL, BMCR conditions. the unevenness of NO concentration was 0.399 131 436%, 0.271 308 784%; the unevenness of NH₃ concentration was 11.431 272 594%, 11.294 855 634%; the unevenness of flue gas temperature was 0.081 935 553%, 0.079 103 890% under 50THA, BMCR conditions, while the coinciding trend of NO and NH₃ concentration decrease at low load. The above indicate that the increasing unevenness of flow field at low load makes a great difference in reducing SCR denitration efficiency, which causes boiler operation, the design of SCR de NO_x system and so on are optimized to decrease the catalyst deactivation rate. **Key words:** SCR, relative standard deviation, denitration efficiency, numerical simulation

结构化填充床内层流流动特性的研究 = **Study of Laminar Flow Characteristics in a Structured Packed Bed**
[刊 汉] LI Nan, SHI Jun-rui, LIU Yang (Key Laboratory of Clean Combustion for Electric Generation &

Heating Technology of Liaoning, Shenyang Institute of Engineering, Shenyang, Liaoning, China, Post Code: 110136) ,LENG Jie (Northeast Electric Power Research Institute co. ,LTD, Shenyang, Liaoning, China, Post Code: 110006) // Journal of Engineering for Thermal Energy & Power. -2016, 31(10) . -79 ~ 83

In this paper, the flow characteristics in structured pellet packed bed was numerically studied in order to quantitatively analyze the flow characteristics in the pore and the effects of the laminar flow in porous media with different particle Re numbers. Results show that when the particle Re is 12.17 and 28.88, the streamline is located on the pellets surface. With the particle Re of 105.57 and 204.74, streamline is no longer on the pellets surface because of the influence of the inertia force. Additionally, there is an obvious backflow in the pore for the case with particle Re of 204.74. **Key words:** porous media, numerical simulation, flow field, packed bed

大型燃煤机组颗粒物与痕量元素的排放特性 = **The Particulate Matter and Trace Elements Emission Characteristics of Large Coal-fired Units** [刊, 汉] PAN Si-wei, ZHANG Kai (Electric Power Research Institute of Guangdong Power Grid Corporation, Guangzhou, China, Post Code: 510080) ,ZHANG Yu, LIU Xiao-wei (State Key Laboratory of Coal Combustion, Huazhong University of Science and Technology, Wuhan, China, Post Code: 430074) // Journal of Engineering for Thermal Energy & Power. -2016, 31(10) . -84 ~ 89

Particulate matter sampling tests were performed after the WFGD on the 1 000 MW and 660 MW units to study the emission characteristics of particulate matter (PM) and trace elements at different conditions. Dekati Gravimetric Impactor (DGI) sample system was used to collect the PMs distinguished to four stages. It is concluded that: the PM emission rises with the boiler due to the increases in the coal consumption and the combustion temperature. The trace elements are evidently enriched in fine particle matter; the enrichment order of trace elements is As > Cr > Pb, proportion to the order of the volatileness. **Key words:** coal-fired unit, particle matter, traces elements, emission characteristic

制药污泥的热解特性及动力学研究 = **Study on Pyrolysis Characteristics and Kinetics of Pharmacy Sludge** [刊, 汉] WANG Shan-hui, LIU Ren-ping, ZHAO Liang-xia (School of Environmental Science and Engineering, Hebei University of Science and Technology, Shijiazhuang, Hebei, China, Post Code: 050000) // Journal of Engineering for Thermal Energy & Power. -2016, 31(10) . -90 ~ 95

The temperature difference-thermogravimetric method was employed to study the pyrolytic characteristics and dynamic law of sludge under different reaction conditions. Results showed that the pharmacy sludge pyrolysis process contains three weight loss stages: loss of moisture, organic matter decomposition and carbonization. The TG and DTG curves under different heating rate (5 °C /min, 10 °C /min, and 20 °C /min) trend are roughly the same. But with the increase of heating rate, TG and DTG curve has a tendency to move to the high temperature area. Flynn-Wall-Ozawa and Šatava-Šesták analysis method was used to explore pyrolysis kinetics of Pharmacy sludge main reaction stage. It was concluded that when the conversion rate is 0.9, the activation energy would be as highest as 150.75